Chapter 13

The Ocean

Over most of the globe the ocean has a rather distinctive vertical structure, with an upper layer ranging from 20 m to 200 m in thickness, consisting of water heated by solar radiation, which is significantly warmer than the underlying deep water. The water in this upper layer is therefore less dense than deep ocean water. This *density stratification* is weak or absent only in certain high-latitude regions of the North Atlantic and in a few other locations. In these regions surface water has become sufficiently cold and salty (via evaporation) to sink into the deep ocean. Such regions therefore convert surface water to deep ocean water. Deep water returns to the surface layer over broad regions of the tropics and subtropics in a manner that is not completely understood. However, it is clear that this transformation must take place by the entrainment of deep ocean water into the surface layer via turbulent mixing processes. The complete circulation, consisting of sinking in selected polar regions, deep transport to the subtropics, entrainment into the surface layer, and surface transport back to the polar regions, is called the *thermohaline circulation*.

13.1 Two-layer ocean

In addition to the thermohaline circulation, there are important horizontal circulations confined within the surface layer. These *gyres* are driven by wind stress acting on the ocean surface. Rather special conditions apply where the surface gyres impinge on the east coasts of continents, which result in poleward-flowing *western boundary currents*. The Gulf Stream off of the east coast of the United States is an example of a western boundary current.

Figure 13.1 shows an idealized model of the ocean structure discussed above. It is unrealistic in a number of respects: In the real ocean the density gradient with depth is continuous and the ocean bottom is not a flat surface. However, these simplifications make the most important characteristic behaviors of the ocean approachable mathematically.

We now approach the problem of disturbances in the real ocean by analyzing the two-layer case illustrated in figure 13.1. For the most part, each layer can be treated separately, in

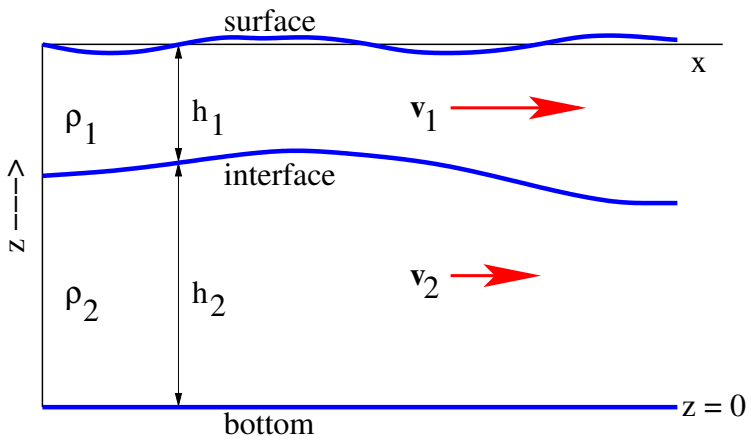

Figure 13.1: Idealized model for the vertical structure of the ocean. The density of the upper layer ρ_1 is less than that of the lower layer ρ_2.

the manner used to deal with the shallow water model. The factor which couples the layers together is the horizontal pressure gradient term.

From the hydrostatic equation the pressure in the first or upper layer is

$$p_1 = g\rho_1(h_1 + h_2 - z), \tag{13.1}$$

where we have assumed that the pressure is zero above the water surface. From this we infer that the pressure at the interface between the two layers is

$$p_I = g\rho_1 h_1. \tag{13.2}$$

Finally, the pressure in the second layer is

$$p_2 = p_I + g\rho_2(h_2 - z) = g\rho_1 h_1 + g\rho_2(h_2 - z). \tag{13.3}$$

The mass continuity equations for each layer are identical to that for a single layer:

$$\frac{\partial h_{1,2}}{\partial t} + \boldsymbol{\nabla} \cdot (h_{1,2}\boldsymbol{v}_{1,2}) = 0. \tag{13.4}$$

Using the fact that $\boldsymbol{\nabla} p_1 = g\boldsymbol{\nabla}[\rho_1(h_1 + h_2)]$ and $\boldsymbol{\nabla} p_2 = g\boldsymbol{\nabla}[\rho_1 h_1 + \rho_2 h_2]$, the momentum equations for the two layers are

$$\frac{\partial \boldsymbol{v}_1}{\partial t} + \boldsymbol{v}_1 \cdot \boldsymbol{\nabla}\boldsymbol{v}_1 + g\boldsymbol{\nabla}(h_1 + h_2) + f\boldsymbol{k} \times \boldsymbol{v}_1 = 0 \tag{13.5}$$

and

$$\frac{\partial \boldsymbol{v}_2}{\partial t} + \boldsymbol{v}_2 \cdot \boldsymbol{\nabla}\boldsymbol{v}_2 + g\boldsymbol{\nabla}[(\rho_1/\rho_2)h_1 + h_2] + f\boldsymbol{k} \times \boldsymbol{v}_2 = 0. \tag{13.6}$$

To understand how this system of equations works, it is sufficient to examine linearized solutions about a state of rest at the earth's equator, where $f = 0$. Letting $h_1 = h_{01}(1 + \eta_1)$ and $h_2 = h_{02}(1+\eta_2)$ and assuming a plane wave moving in the x direction with form $\exp[i(kx-\omega t)]$, the mass continuity equations and the x components of the momentum equations reduce to a set of four linear, homogeneous equations. In matrix form these equations are

$$\begin{pmatrix} -\omega & k & 0 & 0 \\ kgh_{01} & -\omega & kgh_{02} & 0 \\ 0 & 0 & -\omega & k \\ kg(\rho_1/\rho_2)h_{01} & 0 & kgh_{02} & -\omega \end{pmatrix} \begin{pmatrix} \eta_1 \\ u_1 \\ \eta_2 \\ u_2 \end{pmatrix} = 0. \tag{13.7}$$

Taking the determinant of the matrix of coefficients yields

$$\omega^4 - gk^2(h_{01} + h_{02})\omega^2 + g^2k^4(1 - \rho_1/\rho_2)h_{01}h_{02} = 0, \tag{13.8}$$

which has the solutions

$$\omega^2 = \frac{gk^2(h_{01} + h_{02})}{2} \left\{ 1 \pm \left[1 - 4 \left(1 - \frac{\rho_1}{\rho_2} \right) \frac{h_{01}h_{02}}{(h_{01} + h_{02})^2} \right]^{1/2} \right\}. \tag{13.9}$$

In the ocean the fractional difference between ρ_1 and ρ_2 is tiny, which means that $|1-\rho_1/\rho_2| \ll 1$. Using $(1 + \epsilon)^{1/2} \approx 1 + \epsilon/2$, which is valid when $|\epsilon| \ll 1$, equation (13.9) simplifies to

$$\omega^2 = \frac{gk^2(h_{01} + h_{02})}{2} \left\{ 1 \pm \left[1 - 2 \left(1 - \frac{\rho_1}{\rho_2} \right) \frac{h_{01}h_{02}}{(h_{01} + h_{02})^2} \right] \right\}. \tag{13.10}$$

The two solutions are now explored.

13.1.1 External mode

The wave mode associated with the plus sign is called the *external mode*. The term involving the density ratio can be ignored due to its small size, resulting in

$$\omega^2 = gk^2(h_{01} + h_{02}). \tag{13.11}$$

This mode is just like that which occurs for a single shallow water layer of undisturbed depth $h_{01} + h_{02}$. The fact that this layer is made up of two sub-layers of slightly different density is of no signficance here. In the ocean this could be called the "tsunami mode", representing the rapidly moving waves generated by sub-surface earthquakes and landslides. The phase speed of these waves is $c = [g(h_{01} + h_{02})]^{1/2}$, which is very fast for deep ocean basins. This mode is of little interest in climate applications but of great interest for tsunami predictions.

13.1.2 Internal mode

The minus sign in equation (13.10) results in

$$\omega^2 = gk^2 \left(1 - \frac{\rho_1}{\rho_2}\right) \frac{h_{01}h_{02}}{h_{01} + h_{02}} = gk^2 h_e, \tag{13.12}$$

where

$$h_e = \left(1 - \frac{\rho_1}{\rho_2}\right) \frac{h_{01}h_{02}}{h_{01} + h_{02}} \tag{13.13}$$

is the equivalent depth of the internal mode. Note that if $h_{02} \gg h_{01}$ (the usual case), then $h_{01}h_{02}/(h_{01} + h_{02}) \approx h_{01}$.

A significant part of ocean dynamics, especially that part pertaining to climate, is contained in the dynamics of the internal mode. From equation (13.7) we infer that

$$(h_{01} - h_e)\eta_1 + h_{02}\eta_2 = 0. \tag{13.14}$$

This follows from the realization that $\omega^2/k^2 = gh_e$. The displacement of the surface of the ocean is $h'_S = h_{01}\eta_1 + h_{02}\eta_2$ and the displacement of the interface between the two layers is $h'_I = h_{02}\eta_2$. Since $h_e \ll h_{01}$, we have $\eta_1/\eta_2 \approx -h_{02}/h_{01}$ from equation (13.14). Appealing again to equation (13.14), we find that

$$h'_S = h_e\eta_1 = -h_e\eta_2 h_{02}/h_{01} = -(h_e/h_{01})h'_I. \tag{13.15}$$

In other words, the surface displacement is a small fraction h_e/h_{01} of the displacement of the interface between the two layers, and is of opposite sign.

This fact turns out to be very useful for remote sensing of the state of the ocean. Satellite-based radars can measure the vertical displacement of the ocean surface to a high degree of accuracy. This in combination with equation (13.15) allows the vertical displacement of the interface between surface and deep water to be inferred.

Equation (13.7) also yields information about the relative flow velocities in the shallow and deep layers. In particular, we find that

$$u_1 h_{01} = -u_2 h_{02}. \tag{13.16}$$

Thus, the flows in the shallow and deep layers are opposite in direction. The net horizontal mass flux is $\rho_1 u_1 h_{01} + \rho_2 u_2 h_{02}$. Since $\rho_1 \approx \rho_2$, we see that the net horizontal mass flux due to internal mode transports is nearly zero – transport in the shallow layer in a particular direction is compensated by transport in the opposite direction in the deep layer. In the usual case in which $h_{02} \gg h_{01}$, we also see that $|u_2| \ll |u_1|$, i.e., velocities in the surface layer are much stronger than velocities in the deep layer.

This analysis was carried out for the restricted case of linearized gravity waves on the equator. However, to the extent that (a) the density in the surface layer is only slightly

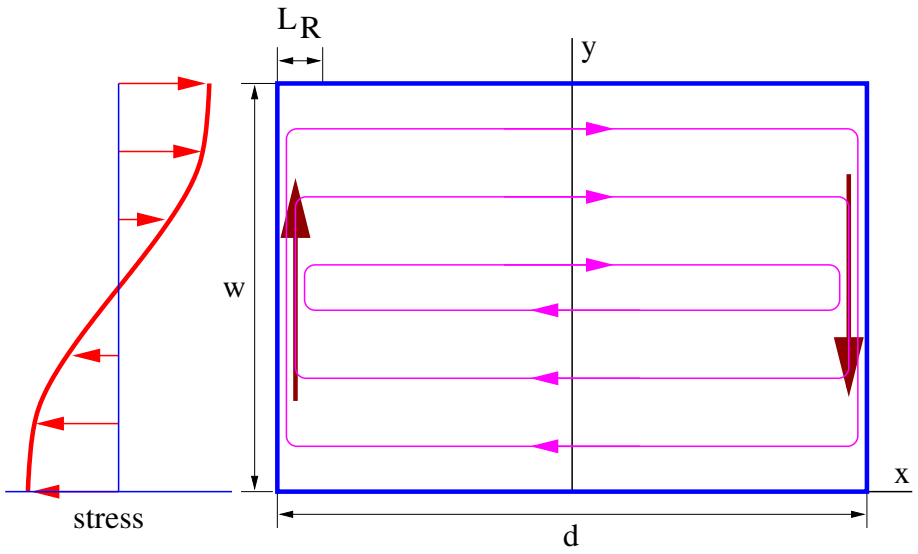

Figure 13.2: Idealized ocean basin with sinusoidal east-west wind stress.

less than the density of deep water, and (b) the thickness of the deep layer is much greater than the thickness of the surface layer, the result is much more general. In particular, the dynamics of the surface layer are essentially the dynamics of a shallow water flow with depth equal to the equivalent depth calculated above. The deep ocean layer responds passively to this mode with only minimal flow velocity, as governed by the condition of zero net mass flux integrated over the depth of the ocean. Under these circumstances, the assumption of a flat ocean bottom, which is highly unrealistic, has no significant effect on the results as long as the thickness of the deep layer greatly exceeds the thickness of the surface layer. Thus, we can carry over the entire apparatus of shallow water flow to the study of internal mode flows.

13.2 Ocean currents

We now explore several examples of real phenomena in the oceans, and how our newly developed tools can be used to understand them.

13.2.1 Wind stress and ocean gyres – f-plane

Let us consider a highly idealized model of an ocean basin with a zonal (east-west) atmospheric wind stress acting on it, as illustrated in figure 13.2. The wind stress pattern is meant to represent approximately that actually found in the northern hemisphere, with surface westerly winds (i.e., *from* the west according to meteorological convection) north of about 30° N and easterly winds south of this latitude. We represent this stress by the cosine

function

$$\boldsymbol{T} = -T_0 \cos(\pi y/w)\boldsymbol{i}, \tag{13.17}$$

where T_0 is a constant. Assuming that the depth of the surface layer of the ocean is $h = h_0(1+\eta)$ where $|\eta| \ll 1$ as usual, we approximate the force per unit mass in the surface layer due to the wind stress as $\boldsymbol{F} = \boldsymbol{T}/(\rho_w h_0)$. The z component of the curl of this force is $\boldsymbol{\nabla} \times \boldsymbol{F} = -[\pi T_0/(\rho_w w h_0)] \sin(\pi y/w)$, and so the potential vorticity evolution equation is

$$\frac{\partial q^*}{\partial t} + \boldsymbol{v} \cdot \boldsymbol{\nabla} q^* = -\frac{\pi T_0}{\rho_w w h_0^2} \sin(\pi y/w). \tag{13.18}$$

where $q = q_0 + q^*$, with $q_0 = f_0/h_0$ as usual.

The perturbation potential vorticity contains a planetary part due to the variation of Coriolis parameter with latitude, and a part due to the motion of the system. Let us initially assume an f-plane, so that the latitudinal variability of the planetary part of the potential vorticity is suppressed. This is highly unrealistic, but the solution to this problem sets the stage for the more complex beta plane case. In this situation the advection term $\boldsymbol{v} \cdot \boldsymbol{\nabla} q^*$ is nonlinear in quantities having to do with the flow of the ocean, and can therefore be neglected in the initial small-amplitude evolution of the ocean circulation which occurs shortly after the surface stress is turned on. In this case we have

$$q^* = -\frac{\pi T_0 t}{\rho_w w h_0^2} \sin(\pi y/w), \tag{13.19}$$

i.e., the potential vorticity initially just decreases in place due to the pattern of wind stress.

The inversion equation for the thickness perturbation is

$$L_R^2 \nabla^2 \eta - \eta = \frac{q^*}{q_0} = -\frac{\pi T_0 t}{\rho_w w h_0 f_0} \sin(\pi y/w) \equiv -\epsilon \sin(\pi y/w), \tag{13.20}$$

where we have encapsulated the expression multiplying the sine function into the single variable ϵ. The solution to equation (13.20) can be divided into inhomogeneous and homogeneous parts, $\eta = \eta_I + \eta_H$. The inhomogeneous part can be written $\eta_I = \eta_{I0} \sin(\pi y/w)$, where $\eta_{I0} = \epsilon/(1 + \pi^2 L_R^2/w^2)$.

We now need to choose a homogeneous solution, i.e., one with ϵ set to zero in equation (13.20), which together with the inhomogeneous solution satisfies the boundary conditions of no flow through the side walls of the ocean basin. Technically, we need to arrange for the normal component of the sum of the geostrophic and ageostrophic flows to be zero on each side wall. However, since the ageostrophic part of the flow is generally small compared with the geostrophic part, we settle for the technically less demanding condition that the component of the geostrophic velocity normal to the boundary be zero there. This condition is satisfied by requiring that $\eta = 0$ everywhere on the boundary.

A solution satisfying this condition is

$$\eta_H = \eta_{H0}\{\exp[-\sigma(x + d/2)] + \exp[\sigma(x - d/2)]\} \sin(\pi y/w), \tag{13.21}$$

where

$$\eta_{H0} = -\frac{\epsilon}{(1+\pi^2 L_R^2/w^2)[1+\exp(-\sigma d)]} \tag{13.22}$$

and where

$$\sigma = \left(\frac{\pi^2}{w^2} + \frac{1}{L_R^2}\right)^{1/2}. \tag{13.23}$$

Recall that the oceanic Rossby radius for the internal mode is of order 50 km, whereas typical ocean basin dimensions (d and w) are thousands of kilometers. This leads to the simplifications that $\eta_{H0} \approx -\epsilon w^2/(\pi L_R)^2$ and $\sigma \approx 1/L_R$.

Contours of constant η are shown in figure 13.2, with arrows showing the flow pattern. The surface layer is thicker in the center of the ocean, consonant with the negative potential vorticity perturbation there. Arrows show the resulting geostrophic flow, which in the interior of the ocean basin tends to follow the pattern of surface stress. However, within a few Rossby radii of the east and west coasts the regime is quite different, with strong thickness gradients and correspondingly strong *coastal jets*, moving southward on the eastern boundary and northward on the western boundary in the northern hemisphere. The circulation in the southern hemisphere has the opposite sense due to the negative value of f_0 there.

As indicated, this solution is only valid for small amplitudes. As the circulation builds up under continuing wind stress, nonlinear effects eventually begin to modify the solution. Ultimately dissipation must begin to counteract the continual buildup of energy in the ocean circulation.

13.2.2 Wind stress and ocean gyres – beta-plane

The initial solution for the case of latitudinally varying Coriolis parameter is identical to the f-plane case. The beta effect only enters when advection of potential vorticity becomes significant. Nonlinear effects enter much earlier in the beta-plane case than for an f-plane, and following the detailed evolution of the flow becomes difficult or impossible. However, it is possible to make significant inferences about the final, equilibrium state of the flow.

In order to get at least a qualitative picture of how the flow evolves in the presence of the beta effect, notice how the eastern and western boundary currents advect the potential vorticity, resulting in a positive potential vorticity anomaly in the eastern current and a negative anomaly in the western current. Both currents have anticyclonic relative vorticity. In the eastern boundary current the positive potential vorticity anomaly creates a positive relative vorticity anomaly, which opposes the relative vorticity anomaly in the jet, reducing the jet strength. Eventually the positive anomaly increases sufficiently to cancel the negative anomaly completely, and the eastern boundary current comes to a halt. On the other hand, the negative potential vorticity anomaly in the western boundary current produces a negative relative vorticity anomaly which reinforces the anomaly pre-existing in the jet. This strengthens the jet, which increases the potential vorticity anomaly, which further strengthens the jet, etc., resulting in a runaway situation.

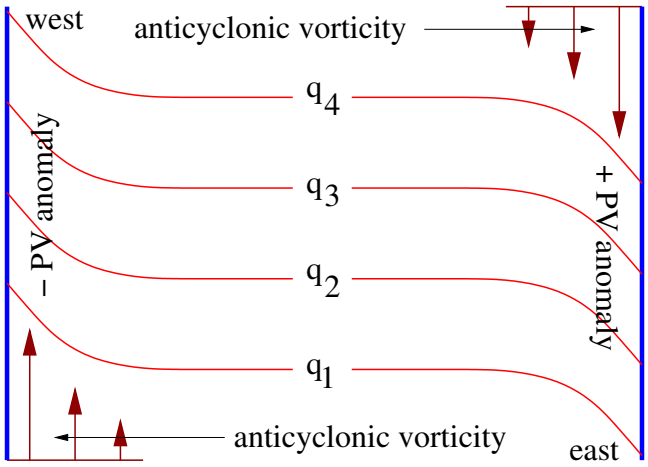

Figure 13.3: Effect of eastern and western boundary currents on potential vorticity distribution. The potential vorticity contours have $q_4 > q_3 > q_2 > q_1$, so that the advection due to the boundary currents causes a positive potential vorticity anomaly in the eastern boundary current and a negative anomaly in the western current.

The kinks in the potential vorticity contours produced in the eastern boundary current propagate to the west as Rossby waves. Rossby wave adjustment continues until the contours become aligned perfectly east-west everywhere except for the western boundary region, where the very strong jet there does not allow equilibration to occur.

When a steady situation is reached everywhere except near the western boundary, the decrease in potential vorticity due to the wind stress curl is counterbalanced by a southward flow. This balance is called *Sverdrup balance* after the Norwegian oceanographer who developed the theory of this phenomenon. In terms of the potential vorticity advection equation, the balance is expressed

$$v\frac{\partial q}{\partial y} = \left(\frac{\partial q^*}{\partial t}\right)_{stress} = -\frac{\pi T_0}{\rho_w w h_0^2}\sin(\pi y/w) \tag{13.24}$$

where q^* is obtained from equation (13.19). Assuming that the thickness of the surface layer does not change much over the ocean, we have $q \approx q_0 + \beta y/h_0$, and the drift velocity is

$$v = -\frac{\pi T_0}{\rho_w w h_0 \beta}\sin(\pi y/w). \tag{13.25}$$

Since the y component of the flow is specified everywhere, the x component can be obtained from the continuity equation, again assuming that $h \approx h_0$. In this case the steady state continuity equation is

$$\frac{\partial u}{\partial x} + \frac{\partial v}{\partial y} = 0. \tag{13.26}$$

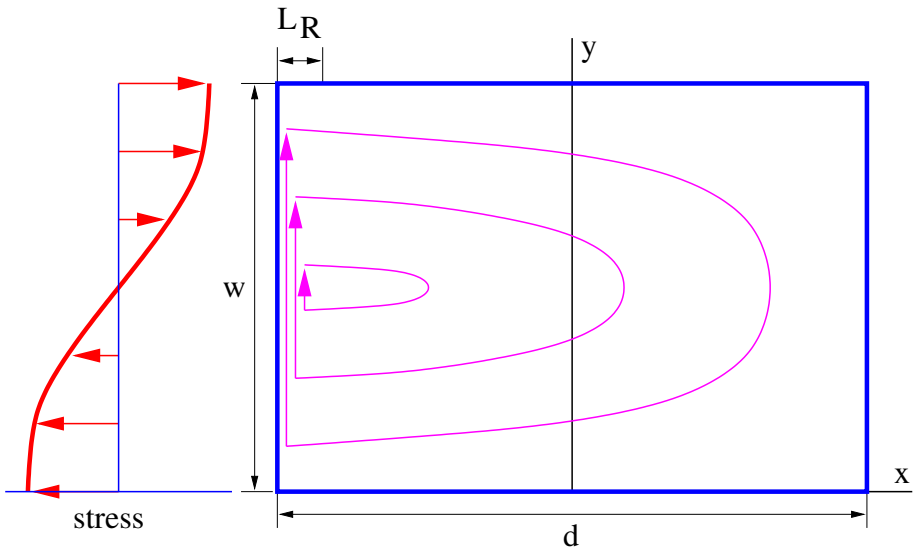

Figure 13.4: Idealized ocean circulation with the illustrated stress. Sverdrup flow occurs in the interior and eastern boundary, whereas western boundary current dynamics applies within a few Rossby radii of the western boundary.

This may be integrated in x to obtain

$$u = \frac{\pi^2 T_0 (x - d/2)}{\rho_w w^2 h_0 \beta} \cos(\pi y / w), \tag{13.27}$$

where we have set the constant of integration (which is actually a function of y) so that $u = 0$ at the eastern boundary as defined in figure 13.2. Notice that $u \neq 0$ at the western boundary. This is because the solution is not valid in the western boundary region itself. In effect, the east-west velocity adjacent to the boundary current serves as a mass sink-source for the current. The resulting circulation is illustrated in figure 13.4.

Comparison with actual ocean circulations shows good agreement with Sverdrup flow and the implied western boundary current flow from the subtropics north to near the axis of the mid-latitude westerly winds. North of this nonlinear effects enter strongly, resulting in a complex, time-dependent structure for the western boundary current.

The real significance of western boundary currents from our point of view is that they transport large quantities of warm water from the subtropics to high latitudes. They are thus key elements in the redistribution of solar heating. The unit of transport volume transport in the ocean is named after Sverdrup: 1 Sv $= 10^6$ m^3 s^{-1}. The Gulf Stream, which is a western boundary current off the east coast of the United States, transports approximately 25 Sv of water from the Gulf of Mexico into the north Atlantic. Further north the transport is even greater.

13.3 References

Vallis, G. K., 2006: *Atmospheric and oceanic fluid dynamics.* Cambridge University Press, 745 pp. Vallis discusses wind-driven oceanic gyres in chapter 14.

13.4 Questions and problems

1. Sverdrup drift and the Gulf Stream:

   (a) Putting in reasonable values for the dimensions of the Atlantic Ocean, the depth of the upper oceanic layer (try 100 m), and the strength of the wind stress, estimate mass of water per unit time drifting south at the latitude of maximum anticyclonic wind stress curl. This equals the northward mass transport in the Gulf Stream at that latitude. Make a reasonable estimate for the maximum wind stress T_0.

   (b) Assuming that the Gulf Stream is one Rossby radius wide, what is the estimated northward flow velocity in the Gulf Stream? Note that the Rossby radius in this case should be based on the equivalent depth rather than the actual depth of the layer, since the entire oceanic gyre is an internal mode involving mainly motions in the upper oceanic layer. You may take the density difference between surface and deep water to be about 4 kg m^{-3}.

2. If the Gulf Stream is 10° C warmer than the main body of the upper ocean, use the results of the above problem to estimate the net northward transport of heat due to the ocean gyre, of which the Gulf Stream is the northward branch. Compare this result to the actual meridional ocean transport of heat. Hint: This transport is equal to the mass per unit time transported by the Gulf Stream times the difference in the internal energy content per unit mass between the northward-flowing Gulf Stream and the main body of the upper ocean. The specific heat of liquid water is about 4200 J kg^{-1} K^{-1}. The seasonally and globally averaged ocean transport of heat toward the poles is about 3×10^{15} W.

3. Ekman drift: Consider a time-independent and spatially uniform wind stress $T_0\boldsymbol{i}$ in the x direction on a two-layer ocean. Assume constant Coriolis parameter. Compute the direction and magnitude of the velocity of the surface layer, which has uniform depth h_0. Assume that the surface stress is distributed uniformly through the surface ocean layer. Hint: This problem is best solved using the momentum equations for the surface layer of the ocean.